Effect of Graphene and its Oxidized Derivatives on Plant Germination and Macronutrients Adsorption

by

Abhishek Kumar

A Thesis Presented in Partial Fulfilment
of the Requirements for the
Degree Master of Science

Approved July 2022 by the
Graduate Supervisory Committee:

François Perreault, Chair
Peter Fox
Abdallah Oukarroum

ARIZONA STATE UNIVERSITY

August 2022

ABSTRACT

The developing world has witnessed a rapid growth in crop production since the green revolution in the 1960s. Even though the population almost doubled since then, food production tripled; most of this growth can be attributed to crop research, fertilizers, infrastructure, and market development. Although the green revolution came with benefits, it has been widely criticized for its negative impact on the environment. The excessive and inappropriate use of fertilizers has led to human and livestock diseases, polluted waterways, loss of soil fertility, and soil acidity. Even though the green revolution was started to ensure food security, it has unintended consequences on human health and the surrounding environment.

This dissertation focuses on the surface characteristics of graphene nanomaterials (GNMs) and their application in agriculture. Among the nutrients needed for crops, some can be easily obtained from the environment (e.g., carbon, hydrogen, oxygen, etc.) while others, like nitrogen (N), phosphorus (P), and potassium (K) often requires supplementation by fertilizers. However, conventional fertilizers have caused problems associated with pH changes in soils, stunted plant growth, and disruption of beneficial microbial processes. The implementation of nano-fertilizers, which can act as controlled-release fertilizers is important. GNMs have shown some promising characteristics for the controlled release of drugs and other chemicals. Therefore, in the first part of this study, the loading capacity of the three macronutrients (N, P, and K) over GNMs of different surface chemistry was characterized. In the second part of this thesis, the effect of graphene oxide (GO) addition on wheat germination was evaluated. Rapid germination is essential for crop establishment to ensure low-cost and high-quality products and keep in check the

sustainable use of resources in commercial agriculture. The results of this thesis indicated that the application GO significantly enhanced the seed germination potential of the wheat crop. It not only increases the root weight but also improves its volume. Future work should focus on the impact of surface chemistry of GNMs on germination which, when combined to the materials' ability to bind nutrients, could help better guide the use of GNMs in agriculture.

DEDICATION

I would like to dedicate my thesis work to my family, especially my dad, Manoj. Dad, thank you for your endless support and belief in me; I would not be here without your love and support. Abhilash, there is no better brother than you. Thank you for guiding me and standing with me through the thick and thins in my life. I would also like to thank my mom, who always taught me to hang on tight, no matter how adverse the situations are. Thank you, guys, for having my back and constantly uplifting me. My family is my strength.

ACKNOWLEDGEMENTS

First, I would like to thank and express my sincere gratitude to my advisor and committee chair, Dr. Francois Perreault, for sharing with me his expertise and allowing working on this project. Dr. Perreault, you have given me invaluable support from the beginning as I started my work and joined the group. Again, thank you for your positive energy and constructive feedback and for guiding me throughout my graduate studies at Arizona State University.

I would also like to extend my gratitude and thank my professors and committee members, including Dr. Peter Fox, for advising me on my research work. My thesis work, your teaching approach for the subject "Environmental Biochemistry and Waste Treatment," really makes it exciting and enjoyable, even though it is one of the challenging subjects for our degree.

I would also like to especially thank my committee member and advisor, Dr. Abdallah Oukarroum, for giving me the support and insights on my research work, especially on the germination assay. Dr. Oukarroum has done and published some great literature on this topic.

Also, I would like to thank all my lab group members for helping me with the lab-related issues because it's a group effort. I extend my special thanks to Houssameddine Mansouri for sharing the germination assay results, Kartik Bhagat and Partho Das for help on FTIR and Zeta potential instrument, and for going with me through vital concepts of this thesis project.

Finally, I would like to acknowledge the Arizona State University School (ASU) of Sustainable Engineering and Built Environment for allowing me to use their laboratory

facilities and employment scope. In addition, I gratefully acknowledge the use of facilities within the LeRoy Eyring Center for Solid State Science at Arizona State University and the financial support from the MORE project for Graduate students.

TABLE OF CONTENTS

CHAPTER Page

LIST OF TABLES

LIST OF FIGURES

Figure Page

CHAPTER 1

INTRODUCTION

Food production has seen many advancements globally, especially in developing countries. One such advancement is the green revolution, which emphasizes increasing food grain production by implementing fertilizers in agricultural fields (Pingali, 2012). The World Bank applauded the introduction of green agriculture as it aimed to reduce rural poverty and improve worldwide food security. However, even though the green revolution was a success, World Bank's report indicated that the population's health was not improved (John & Babu, 2021). One reason the organization gave was the excessive leaching of nutrients from fertilizers into freshwater bodies (Choudhary et al., 2018). Another observation was that the crops used in the green revolution were water-intensive, resulting in increased stress on freshwater supplies in many developing countries (Kayatz et al., 2019).

Most of the nutrients in conventional fertilizers are water-soluble (Mayhew, n.d.), resulting in leaching and run-off of nutrients, particularly when placed in acidic sandy soils or under heavy rainfall conditions (Zhang, 2017). A higher amount of fertilizers are used to overcome this problem, thus exacerbating the environmental impacts. Furthermore, as the constituents of conventional fertilizers reach the water body, the released nutrients encourage the growth of microorganisms, thereby reducing the dissolved oxygen content of the water bodies. Also, runoff from agricultural fields, especially nitrogen nutrients, leads to higher ammonia in the aqueous system. This higher ammonia content leads to ammonia toxicity of aquatic life and can eventually cause a change in species life (Berg, 2017).

Implementing nanotechnology in agriculture started with the realization that conventional farming techniques will neither increase crop production nor restore the ecosystem damaged by existing farming systems (Mukhopadhyay, 2014). The unique properties of nanomaterials at the nanoscale make them potential candidates for developing novel tools supporting sustainable agriculture (Fraceto et al., 2016). Recently, a wide range of possible nanotechnology applications has been anticipated, such as nano fertilizers, nano pesticides, biosensors, and nano-enabled remediation of contaminated soil (Usman et al., 2020). The development of controlled-release fertilizers (CRFs) is particularly interesting, making the nutrients available to plants slower than conventional fertilizers. As a result, CRFs can boost crop efficiency by sustained adding mineral shortage to the soil and decreasing fertilization frequency, lowering costs, and reducing pollution (Kabiri et al., 2017).

Graphene nanomaterials (GNMs) are carbon-based NMs investigated for their various environmental applications, particularly in water and wastewater treatment (Song et al., 2018); (H. Wang et al., 2020); (Ersan et al., 2017). Previous studies have suggested that GNMs can be effective loading platforms for macro-nutrients (Kabiri et al., 2017). Another study pointed out that GNMs have a large specific surface area and physically interconnected porous network (Gadipelli & Guo, 2015), making GNMs a viable option for nano fertilizers. Graphene (GP, GS) is a monolayer of carbon atoms covalently bonded in a sp^2 arrangement in its unblemished condition. Oxidized forms of graphene, such as graphene oxide (GO) or reduced graphene oxide (rGO), also exists, with varying degree of oxygen atoms in the carbon structure. When graphene changes to GO, the properties of the material change from hydrophobic to hydrophilic as the number of

hydrophilic sites increases due to the rise in oxygen binding site. The structure of GO can be defined as a sheet-like structure with a high density of oxygen functionalities such as carboxyl, hydroxyl, epoxy, and carbonyl groups present at the binding site of the carbon lattice. The tendency of these oxygen functional groups to agglomerate and form a highly oxidized domain while surrounded by pristine graphene structures is a critical factor for the aqueous stability of GO (Zhou & Bongiorno, 2013). The structure of rGO is intermediate between GO and GS and is obtained by the chemical or thermal reduction of GO to remove the oxygen functional groups. The reduction process is never entirely successful at restoring the sp^2 structure; therefore, the properties of rGO lie between GO and rGO, with partial hydrophilicity. Figure 1 below shows the GNMs and their structural differences

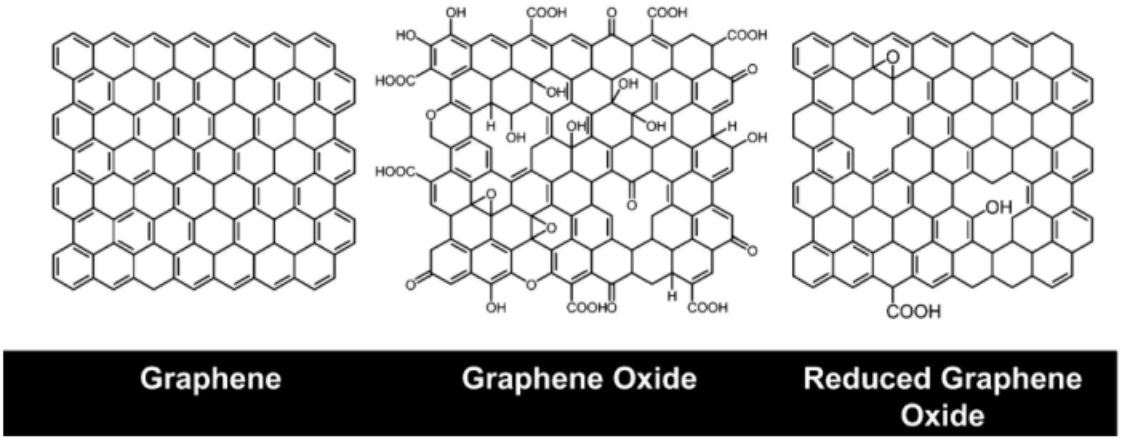

Fig 1. Overview of Different GNMs Based on their Oxygen Content. Figure retrieved from Perreault, De Faria, et al., 2015

Moreover, some of properties of GNMs that are of a lot of interest for the implementation of this project, like higher surface area and easier functionalization of GNMs will facilitate the loading of macro-nutrients over it. Also, properties like higher

resistance and light weight will reduce the frequency of replacement of the platform. In the later stage of this project, it is being implemented in soil, so the anti-microbial properties of GNMs will help prevent nearby biological activities in the normal functioning of the platform.

In this project, we will be looking at GNMs as nano fertilizers as they have shown controlled release potential and characteristics suitable for their implementation in the agricultural fields. To comprehensively understand the performance of nano fertilizers, we are looking at how the nutrients will behave at the interface of the GNMs with the help of adsorption experiments. Due to the varying number of oxygen functional groups as potential binding sites for ions, we will investigate the effect of the oxygen content on nutrient adsorption by GNMs. Many studies have suggested using GO as an adsorbent for heavy metal removal from water due to its high oxygen content (Kabiri et al., 2017). Therefore, a fundamental postulate in this work is that the oxygen content will influence the capacity of GNMs to sorb nutrients in fertilizer's formulation.

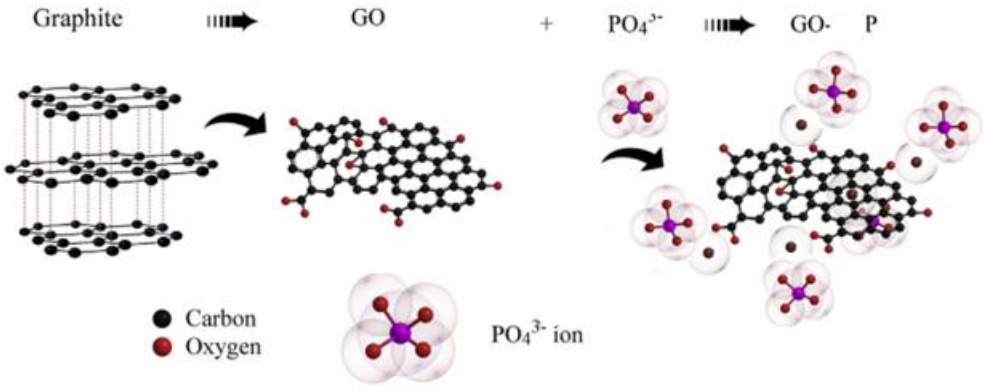

Fig 2. Schematic showing the interactions between the nutrients and GO. Adapted from Andelkovic et al., 2018.

For the second chapter of this project, we were interested in the in-field application of GNMs in agriculture. We performed a germination assay on wheat crops in the presence of GO, where the hydrophilicity and water transporting properties of GO are exploited to obtain better germination outcomes. Several germination studies have been conducted using NMs, showing a wide range of results. For example, Ag NPs, have been observed to inhibit barley, ryegrass, and cucumber germination (El-Temsah & Joner, 2012); (Zhou & Bongiorno, 2013); (Barrena et al., 2009), although NPs containing Ag, ZnO, or Si have no effect on *Cucurbita pepo* germination (Stampoulis et al., 2009). *Brassica juncea* is greatly aided when the concentration of AgNPs is around 25 ppm and TiO2 NPs administering the germination of aged spinach seeds (Arora et al., 2012); (Nile et al., 2022). Furthermore, CNTs have been discovered to increase tomato germination and growth by penetrating the seed coat and increasing the expression of the water-channel gene (Khodakovskaya et al., 2009); (Madhurani et al., 2011).

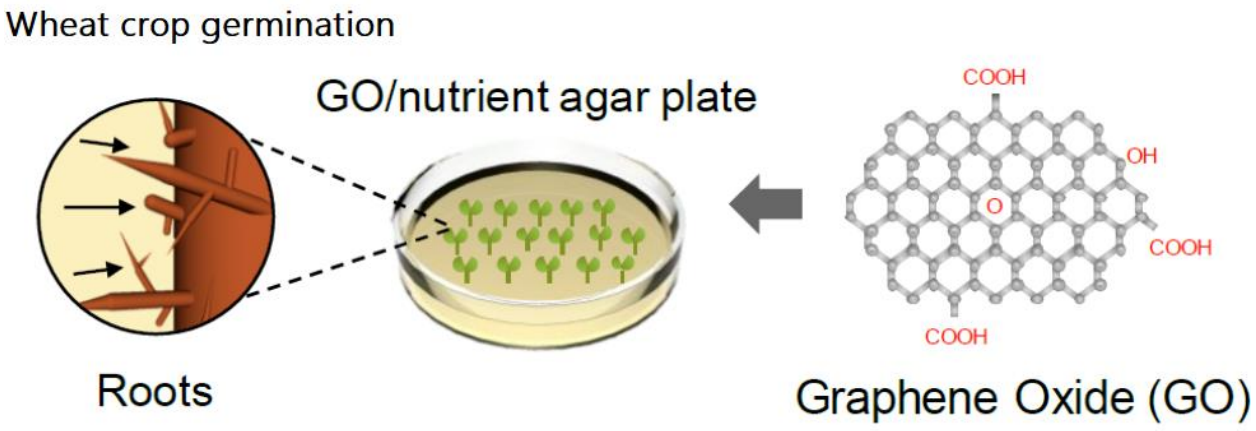

Fig 3. Simple schematics showing the steps in the germination study of Wheat Crops in presence of GO. Adapted From Park et. al. 2020.

Overarching goals and needs. The application of GNMs has been of interest in several sectors for the past two decades. Also, the macro-nutrients are the needs of plants for their optimal growth. In the first chapter of this project, we are trying to understand the loading of different nutrients over GNMs so that they can be utilized in the agricultural field for a sustainable solution as nano fertilizers. In addition, in the second chapter, we will be looking at the effect of GO on weight and the volume of the root of wheat crops during germination at different concentrations. At last, we will be examining the change in the chlorophyll content of the crop in the presence of GO.

Research Question and Hypothesis

Q1) Can Graphene and its oxidized derivatives provide a platform for the macronutrients to be adsorbed?

Q2) At what GO concentration will the wheat crop germination rate will be highest?

Hypotheses:

H1) The surface chemistry of GNMs will play a dominant role in GNMs-macronutrient interaction, and adsorption will be governed by the overall surface charge of the nutrients and materials.

H2) There should be a concentration of GO at which the rate of growth of the wheat seedling is highest as compared to other concentrations, showing germination rate does not increase with an increase in GO concentration.

The following research objectives were pursued to verify the above hypotheses:

1. Preparation of the suspended samples of different GNMs of different oxygen content in Deionized (DI) water solution
2. Characterization of the surface of prepared samples of GNMs
3. Quantify the adsorption of nutrients on GNMs using isotherm adsorption experiments.
4. Investigate the germination of wheat in the presence and absence of GO sheets.

Chapter 2

Background Literature

2.1 Application of Graphene and its oxidized derivatives nanomaterials (GNMs)

Graphene has become one of the trending topics in the research field this decade. It can be attributed to some of its properties like high specific surface area, surface charge, mechanical strength, electron mobility, and high thermal conductivity (Madurani et al., 2020). Because of this unique behavior, graphene was implemented in numerous fields like electrical, biomedical, agriculture, and construction (Perreault, Fonseca De Faria, et al., 2015). Graphene has broad development prospects in areas like seawater desalination, water purification, air pollution detection and control, and agricultural remediation (Aacharya & Chhipa, 2020); (Cohen-Tanugi & Grossman, 2015); (Xiong et al., 2015). Because of its higher surface area, graphene is expected to be a desirable candidate to replace traditional adsorbents in environmental pollution control (Rashed, 2013).

The second material investigated in this work is GO. Even though GO has similar structures to graphene, they are very different in terms of their properties. The reason for this is the presence of varying oxygen groups found on the carbon structure. For example, due to free electrons, graphene has several applications in the electronics industry as a superconductor. In contrast, GO acts like an electron insulator (Chu, n.d.). However, adding oxygen functional groups provides GO with other properties of interest for environmental applications, such as higher aqueous stability, high adsorption capacity for ionic species, and higher biocidal potential (Faria et al., 2018); (Ersan et al., 2017). The latter was shown to be very species-dependent, with some species showing higher toxicity

of GO over graphene while others showed the opposite trend (Barrios et al., 2021). Because of these characteristics, GO has applications in sectors with membranes, coatings, photocatalysis, and solar cells (Perreault, Fonseca De Faria, et al., 2015); (Inurria et al., 2019); (Li et al., 2010).

The third adsorbent considered for this study is rGO, the reduced form of GO. The production of rGO debuts with GO formation through chemical oxidation, which is then reduced chemically or thermally to restore the sp^2-bonded structure (Chua & Pumera, 2013). Depending on the degree of reduction, the properties of rGO can be between superconductors and insulators. The applications of rGO range from fields like electronics and energy storage to environmental or biomedical applications, in controlled delivery systems for example (Compton & Nguyen, 2010).

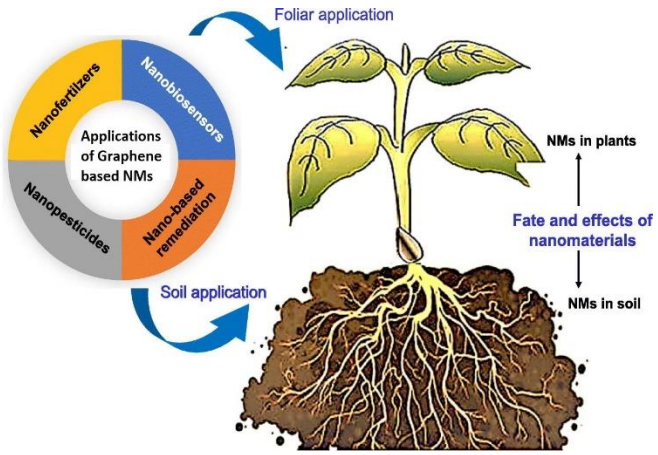

Fig. 4. Various applications of GNMs in agriculture as well as the fate and effects of GNMs in soil and growth of plants. Adapted from Usman et al., 2020.

2.2 Application of macronutrients in the development of crops

For the optimal growth and development of plants, the availability of macro-nutrients is one of the primary requirements. Therefore, N, P, and K are essential elements

of any fertilizers. These nutrients are also referred to as the “Big 3” in commercial fertilizers (Lines-Kelly, n.d.). Among the three macronutrients, N is considered the essential nutrient and is absorbed by the plants in the highest proportion. One main reason is that N is critical to forming proteins, the building blocks of the cells in all living organisms. The second of the “Big 3” is P, which is crucial for the ability of the plant to use and store energy, including photosynthesis. K is the third key nutrient for the plants and is used to increase the plant’s resistance to diseases, which is vital for the quality of the crop yield.

Even though N nutrient is required in the maximum amount, insufficiency in any nutrient required can be devastating for the health of the plants and eventually will be reflected in the overall plant yield (The Fertilizer Institute, 2014). Some of the symptoms of N deficiency in plants are 1) stunted crop growth, 2) chlorosis on leaves (light green to yellow foliage) 3) weakness during the flowering and fruiting, which results in lower yields. Likewise, the deficiency of P symptoms are 1) stunted growth, 2) weak roots, 3) thin shoots, and 4) dark green, purple, or red leaves. Also, the K deficiency in the plant causes reduced growth, yellowing or burning of the leaf margins, and dead spots on older leaves (Hajdu, 2019). This project will deal with the three primary macronutrients (N, P, K).

2.3 **Nano-fertilizer**

Although using chemical fertilizers increases crop productivity, they have caused an imbalance in the mineral content of the soil. In addition, they have caused irreparable damage to soil structure and microbial flora. Again, due to the growing global population, there are expectations of ever-increasing food and grain supplies, which results in a need

to rely on synthetic fertilizers. The application of nanotechnology in agriculture has demonstrated its ability to support sustainable agriculture by tailoring fertilizer production. By the use of nano-fertilizers, plant nutrition, nutrient efficiency, and soil fertility are enhanced. According to the type of formulation, nano fertilizers are classified into three subcategories: 1) Nanoscale fertilizer, 2) nanoscale additive and 3) nanoscale coating of fertilizers (Mejias et al., 2021). A study suggested that $CuSO_4$ and $ZnSO_4$ fertilizers were dissipated in the first 20 hours of application compared to GO-based nano-fertilizers, which showed 55% release in the first 72 hours (Kabiri et al., 2017). In another study of GNMs, it was observed that when GO was used as the coating material on fertilizers, the fertilizers showed CRF behavior compared to the fertilizers used without any coating (Andelkovic et al., 2018). Another study addressed the concern of accumulation of NMs in the crops; it was pointed out that GNMs, when applied to the soil as fertilizers, will not leach to the crop due to the carbon-carbon bonding. (He et al., 2018).

2.4 Germination Assay

Even though nanoparticles are currently used in different aspects of agriculture, the use of NMs in the growth of plants and modulating their physiological response is a relatively recent practice (Prakash & Chung, 2016). Some studies also suggested that nanotechnology has the potential to revolutionize the agricultural industry and plays a vital role in food and crop production (Mukherjee et al., 2016). Several studies support this premise; a study that was done to observe the effect of ZnO NPs on the germination assay of wheat showed a significant favorable influence on the seed germination performance compared to the seed with no exposure to NPs. The study also pointed out that the seedling water uptake was improved due to the presence of ZnO NPs (Rai-Kalal & Jajoo, 2021).

Similarly, a study suggested that ZnO NPs improved the number of roots, plant biomass, and overall growth of shoots and leaves when used in the germination of wheat crops (Awasthi et al., 2017). Another study done on Ag NPs were used for the germination assay of tomato seeds, advised that NPs have a significant effect on seed germination rate, germination speed index, and development of the stem, root systems, photosynthesis pigments, and enzyme activities (Salih et al., 2022). Seed priming with NPs might be a cost-effective and environmentally beneficial smart farming strategy. Adopting this innovative farming approach could help the agricultural sector achieve its goal of improving seed germination and overall crop productivity in the future.

CHAPTER 3

MATERIALS AND METHODS

3.1 Materials and chemicals

The adsorbent materials graphene powder (GP), GO, and rGO were purchased from the ACS materials, Walnut Street, California. The graphene sheet (GS) was obtained from Graphene Supermarket (Ronkonkoma, NY). The adsorption testing kits for testing the nutrients N, P, and K were purchased from Hach Company (Loveland, CO). The adsorbate chemicals Ammonium Nitrate (NH_4NO_3), Potassium Bicarbonate ($KHCO_3$), and Potassium Di-hydrogen Phosphate (KH_2PO_4) were obtained from Sigma-Aldrich, St. Louis, MO. For the germination assay, the crop seeds were obtained from a local Ben Guerir, Morocco store. All the chemicals used for the project were of ACS grade and higher. All the solutions were made, and surfaces were cleaned using deionized (DI) water from a BarnsteadTM GenPure xCAD Plus Ultrapure Water Purification System (Thermo Scientific, Waltham, MA), and the surfaces were wiped using Kim wipes.

3.2 Nanoparticles characterization

3.2.1 Raman Spectroscopy

For Raman spectral analysis, GNMs were prepared with 2 mg/mL concentration, using DI water in 20 mL glass vials. The glass vials are then placed in a bath sonicator for 2 hours. After sonication, samples were transferred on glass slides by placing a ~10 µL drop on the glass slide and letting it evaporate. Evaporation was accelerated by placing the glass slide on a hot plate for rapid evaporation. The process was repeated until a sample thickness of around 5 µm was obtained on the glass slide. Raman spectra were measured

using a custom-built Raman spectrometer operating with a 532 nm laser in a 180° geometry at the Eyring Materials Center at ASU. Measurements were performed on the glass slide having the samples and accumulation time of 10 s. Each Raman spectra depicted is the average of three replicate samples. After the sample measurements were completed, the results were baseline corrected using the concave rubber band method. The results were further analyzed with the help of OriginPro software (2018 64-bit). The D/G Ratio was calculated as an indicator of the defect density in the material, using the ratio between the G (1590 cm^{-1}) and D (1350 cm^{-1}) bands, as previously described (Perreault, De Faria, et al., 2015).

3.2.2 Fourier Transform infrared (FTIR) spectroscopy

For the FTIR spectroscopy, the analysis was done with the help of attenuated total reflection mode (ATR-FTIR), and the sample preparation method was similar to that of Raman spectroscopy. FTIR analyses were done using a Nicolet iS50 ATR-FTIR with 4 cm^{-1} resolution, 128 scans/sample, and equipped with a diamond type IIa crystal. Due to band broadening and/or band shifting in the infrared spectra caused by different GNMs, all spectra were baseline corrected with the same amount of baseline points and only shifted where necessary (no more than 5 cm^{-1}).

3.2.3 X-ray Photoelectron spectroscopy

The sample holder was covered with a double-sided copper tape for XPS analysis and dusted with enough GO powdered material(Cruces et al., 2021). X-ray photoelectron spectroscopy (XPS) was performed on a VG 220i-XL (Thermo Fisher Scientific Ltd. Hampton, NH) equipped with a monochromatic Al K-alpha X-ray source. XPS was used

to quantify the carbon to oxygen (C:O) ratio, and data were analyzed using the CasaXPS software (version 2.3.18).

3.2.4 Zeta Potential

The Zeta potential characterization was performed on a NanoBrook 90Plus PALS. The GNMs samples were prepared with 1 mg/mL initial concentration and sonicated for 1.5 hours. Then, the samples were diluted further by 1/50 factor using an electrolyte solution of 5 mM KCl and 0.1 mM HCO_3. The basic and acidic solution was used as an electrolyte for measuring samples to ensure no artifacts were involved in the solution because of the surface reaction during measurement. With the electrolytic solution, analysis and measurements were taken over a pH range from 6-10 and step durations of 30 to 60 seconds to determine the zeta potential of each sample.

3.3 Graphene NMs Batch Adsorption experiment

All the adsorption experiments were done using a colorimetric approach, which works on the principle of Beer-Lambert Law, stating that the solute's concentration is proportional to absorbance (Clark, 2022).

3.3.1 Nitrogen/Nitrate nutrient testing

For the N nutrient testing, the samples of GNMs of an initial concentration of 2 mg/mL were prepared with DI water in clean glass vials. The samples were then bath sonicated for 2 hours. On the sides, the adsorbate sample, of NH_4NO_3, of concentration 64 mg/L was prepared. The adsorption experiment was conducted at five diluted adsorbate concentrations, namely, 4 mg/L, 8 mg/L, 16 mg/L, 32 mg/L, and 64 mg/L for each adsorbent of GNMs. The next step was to remove the glass vials from the sonication, and

the adsorbate was added to the GNMs. For the adsorbate addition, we followed the values in table 1. After the adsorbate addition, we added DI to the glass vails so that the final concentration of the GNMs in the solution was 1 mg/mL:

Table 1. Combination of volumes of adsorbate and DI water added to test samples to maintain fixed concentration of adsorbate in sample, for N and P nutrients

Contaminant concentration (mg/L)	Volume of nutrient (mL)	Volume of DI (mL)
64	8	0
32	4	4
16	2	6
8	1	7
4	0.5	7.5

After this step, the glass vials surface is cleaned properly with Kim wipe papers, wrapped with aluminum foils, kept on a shaker, and agitated for 48 hours at a constant speed of 320 rpm (Kim et al., 2015). After 48 hours, the samples were removed from the shaker and unwrapped.

Before adding the colorimetric reagents, the GNMs were removed by filtration using a syringe filter. The filtration step is essential because GNMs have their color in the sample, which would cause interference in the measurement if not removed. The size of the filter used to remove GS and rGO from the sample was a 0.2μm pore size, and for GO, the filter used was 0.45 μm in pore size.

After the syringe filtration was completed, we followed the Nitrate TNTplus Test manual procedure to measure N left in the solution. Afterward, the glass vials were transferred to the Hachtesting vails. In the case of N, the measuring wavelength is 345 nm**.**

3.3.1.1 Overview of the reaction involved in the nitrate testing kit

Step 1. Nitrate ion in the presence of sulfuric acid produces nitonium ion and HSO_4^-

$$NO_3^- + H_2SO_4 \longrightarrow NO_2^+ + HSO_4^-$$

Step 2. Nitronium ion is **electrophilic** and attacks aromatic ring of **di-methyl phenol** to form **nitro-carbonium ion**

Step 3. HSO_4^- extracts hydrogen ion from nitro-carbonium ion to form **Nitro dimethyl product**

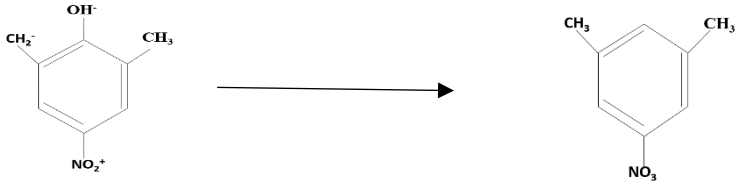

Step 4. Nitro-dimethyl products are **highly colored** (the color produced is dependent on the nitrogen functional group)

3.3.2 Phosphorus/phosphate nutrient testing

The sample preparation and measurement for reactive P nutrient is similar to the nitrate testing method. After following the procedure specified in the Hach manual of TNT 843, we get the P nutrient in the samples after the completion of the adsorption experiment. The wavelength at which Phosphorus measurement was done in the HACH Testing machine is 880 nm.

3.3.2.1 Overview of Reactive Phosphorus Testing Kit

Step 1. The reactive or orthophosphate ions react with molybdate and antimony ions in an acidic solution to form an antimonyl phosphomolybdate complex

$$PO_4^{3-} + MoO_4^{2-} + Sb^{3+} \longrightarrow (Sb)_3PMo_{12}O_{40}$$

Step 2. antimonyl phosphomolybdate complex is reduced by ascorbic acid to phosphomolybdenum blue.

$$(Sb)_3PMo_{12}O_{40} \xrightarrow{C_6H_8O_6} P_9[Mo_{154}O_{462}H_{14}(H_2O)_{70}]$$

Step 3. The formation of phosphomolybdenum blue is proportional to the amount of Phosphorus present in the solution

3.3.3 Potassium nutrient Testing

The sample preparation for K nutrient testing is slightly different from that of the N and P nutrient testing procedures because the sample volumes should be 25 mL as specified in the manual testing kit. However, we adjusted the volume of adsorbates and adsorbents, so the initial concentration of 2 mg/L and a final concentration of 1 mg/L of samples was maintained, the same parameters as that of N and P nutrients testing:

Table 2. Volume of $KHCO_3$ solution and DI water added to test sample to maintain specific concentration of adsorbate in the sample

Contaminant concentration (mg/L)	Volume of nutrient (mL)	Volume of DI (mL)
64	12.5	0
32	6.25	6.25
16	3.125	9.375
8	1.5625	10.9375
4	0.78125	11.71875

After the incubation period of the adsorption experiment, the samples were filtered using the syringe filtration technique as mentioned above in the N nutrient testing (section 3.3.1). Then, we followed the instructions given in the testing manual for the potassium reagent set to get the amount present in the solution, which can be further used to give the amount of nutrient adsorbed over the GNMs.

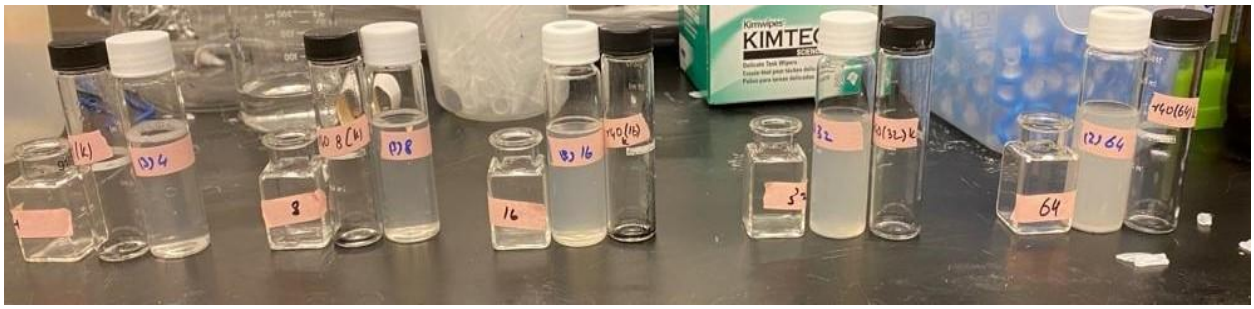

Picture 1. The picture was taken during adsorption testing of GO versus K. The color of the solution changes is proportional to the adsorbate in the solution after completion of the adsorption experiment

Step 1. Potassium in the sample reacts with sodium tetraphenylborate to form potassium tetraphenylborate, an insoluble white solid.

$$K^+ + (C_6H_5)_4BNa \longrightarrow (C_6H_5)_4BK + Na^+$$

Step 2. The amount of insoluble white solid is proportional to Potassium present in solution[37]

3.4 Germination Assay

Four different suspensions of GO in DI were prepared for the germination assay, namely 20 mg/L, 40 mg/L, 60 mg/L, and 80 mg/L. The suspensions were made in glass vials placed in an ultrasonicator bath (ELMASONIC S100) for two hours. After this, four Petri dishes having Whatman paper were set up for each concentration, and these Whatman

papers were soaked in 5 mL of DI water to keep the moisture content high. After this step, ten seeds of wheat crops are evenly distributed in each petri dish and placed in obscurity until the germination cycle is completed; in this case, the period was of 3 days. After the germination cycle, a visual inspection was done, and the seedlings that showed radicle and embryonic shoot (coleoptile) coming out of the seed coat were considered germinated. Most seeds showed germination after the germination period and the ones that did not were discarded. Then, the dishes were placed in an alternate cycle of 8 hours of dark and 16 hours of light for the next 18 days; in the process, the Petri dishes received 3 mL of respective concentrations of GO doses every day for the next seven days. After seven days, two seeds from each petri dish are transferred in a hydroponic test set up consisting of a 50 mL tube covered in foam. The hydroponic tubes had 50% of Hoagland medium for the initial two days. Then, the solution was replaced with a full-strength Hoagland solution for the rest of the analysis, where the solutions were replaced after five days.

A similar study was done in 2019, where effect of GO was observed on rice crops with the help of germination. After doing the initial cleaning of the crop seed with 3% Hydrogen peroxide and DI water, the seeds were placed in an incubator at 28^0 C. Similar to our study, the seeds were checked for germination after 24 hours, and the sprouted seeds were then transferred to Petri dishes with filter paper, DI water, and GO at different concentrations. Seeds were then exposed to an alternate cycle of 16 hours of light to 8 hours of darkness. After the completion of 16 days of treatment, further measurements were done on the seeds(Chen et al., 2022). Another study was done to observe the germination effect of GO in the ontogenetic stage of *Triticum aestivum L.* seedlings. Initially, the surface of wheat seeds was cleaned with 1% sodium hypochlorite and DI

water. Similar to our study, three setups were prepared with GO at different concentrations to measure the GO effect; the fourth was DI water, which served as the control for the experiment. The seed germination was prepared in Petri dishes (20 seeds in each petri dish and four Petri dishes for each sample) with filter paper and kept in a controlled environment for 48 hours. After that, the Petri dishes were transferred to plant growth chambers for the next five days, where the seed was exposed to alternate exposure to 16 hours of light to 8 hours of dark the next five days. Also, GO was replenished in the Petri dishes at regular intervals. After the completion of 7 days, further measurements of the seeds were done (Vochita et al., 2019).

CHAPTER 4

RESULTS AND DISCUSSIONS

4.1 Material characterization

4.1.1 X-ray photoelectron spectroscopy (XPS)

XPS is a surface-sensitive quantitative spectroscopic technique based on the photoelectric effect that accurately estimates chemical species in GBNMs. The XPS data is used to estimate the defects' quality and helps differentiate between the GNMs and other oxygen-derivatives. This XPS analysis allows us to quantify the graphitic carbon sp^2, defects sp^3 carbon, carbons bonded to hydroxyl and epoxy groups, and carbonyl and carboxyl groups.

The analysis of the results and the XPS spectra can be accessed in Fig 6. As mentioned, the peaks deriving from sp^2 and sp^3 carbon have different C1 s signals in the XPS analysis. Below is the compiled XPS data representing the atomic percent of the carbon, oxygen content, and relative atomic percentage of carbon-oxygen functional groups determined from the component fitting of the C 1s envelope for graphene samples. It can also be observed from the XPS spectral analysis, GP has the highest percentage of carbon content, and GO has the highest oxygen content among the three graphene samples.

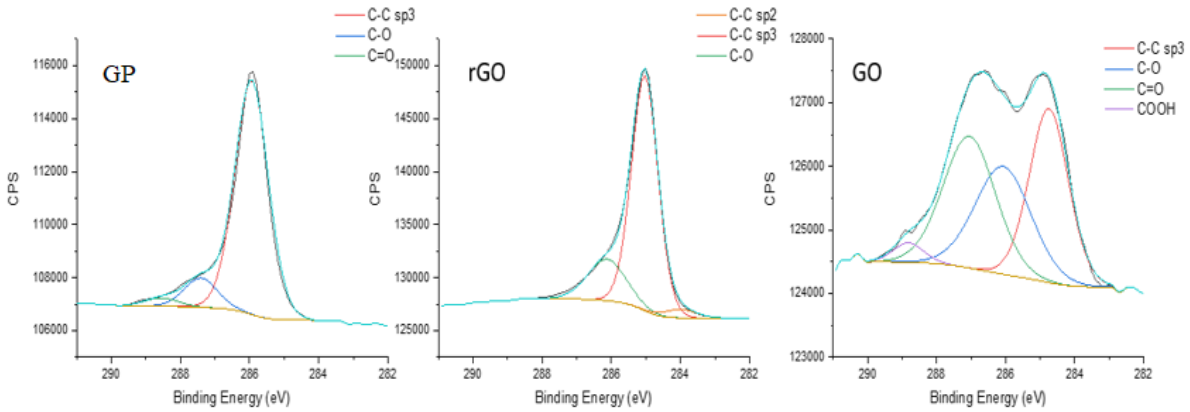

Fig 5. The C1s peak deconvolution of the XPS spectra of GP, GO, rGO, showing the different types of functional groups on the GNMs used in this study.

Table 3. Compiled XPS Data Representing the Atomic Percent of the Carbon and Oxygen Content and the C/O Atomic Ratio. Determined from the Component Fitting of the C 1s Envelope. Different Letters Represent Statistical Significance Between Materials at $p \leq 0.05$ (n=3)

	% C	**% O**	**C/O**	**% C-C sp^2**	**% C-C sp^3**	**% C-O**	**% C=O**	**% COOH**
GP	94.7	5.65	16.7	n.d.	86.2	10.7	3.07	n.d.
rGO	91.7	7.25	12.6	3.37	77.2	19.5	n.d.	n.d.
GO	72.7	27.3	2.66	n.d.	33.5	29.6	33.9	2.91

n.d = not detected

4.1.2 Raman Spectroscopy

To verify the chemical structures and the type of bonds present in GNMs, we used Raman Spectroscopy. The results from the spectral analysis showed two significant peaks "D" band at 1341 cm^{-1} and the "G" band at 1595 cm^{-1} (Ghann et al., 2019). The D band can be accredited to the presence of oxygen functional groups like hydroxyl, carbonyl, carboxyl, and epoxy groups, where the presence of G bands in the samples showed carbon-

carbon bonding in the GNMs. We anticipated similar results for the Raman spectroscopy, in case of GO and rGO samples. But analysis of rGO showed that the D peaks are higher than that of GO, suggesting that more isolated graphene domains were present in rGO due to the lower amount of oxygen groups present as compared to GO after reduction(Hidayah et al., 2017). When the analysis done on GP, it showed the presence of D peaks higher than G peaks in the materials, indicating higher oxygen content, making it an unsuitable candidate for adsorption experiments (Sheka et al., 2020). We also performed Raman spectroscopy analysis for GS, it showed a weak D band, fewer defects in the sample, and a prominent G band at around 1591 cm^{-1} establishing the presence of sp^2 bonded carbon atoms. So, we decided to conduct the adsorption experiments using GS samples rather than GP.

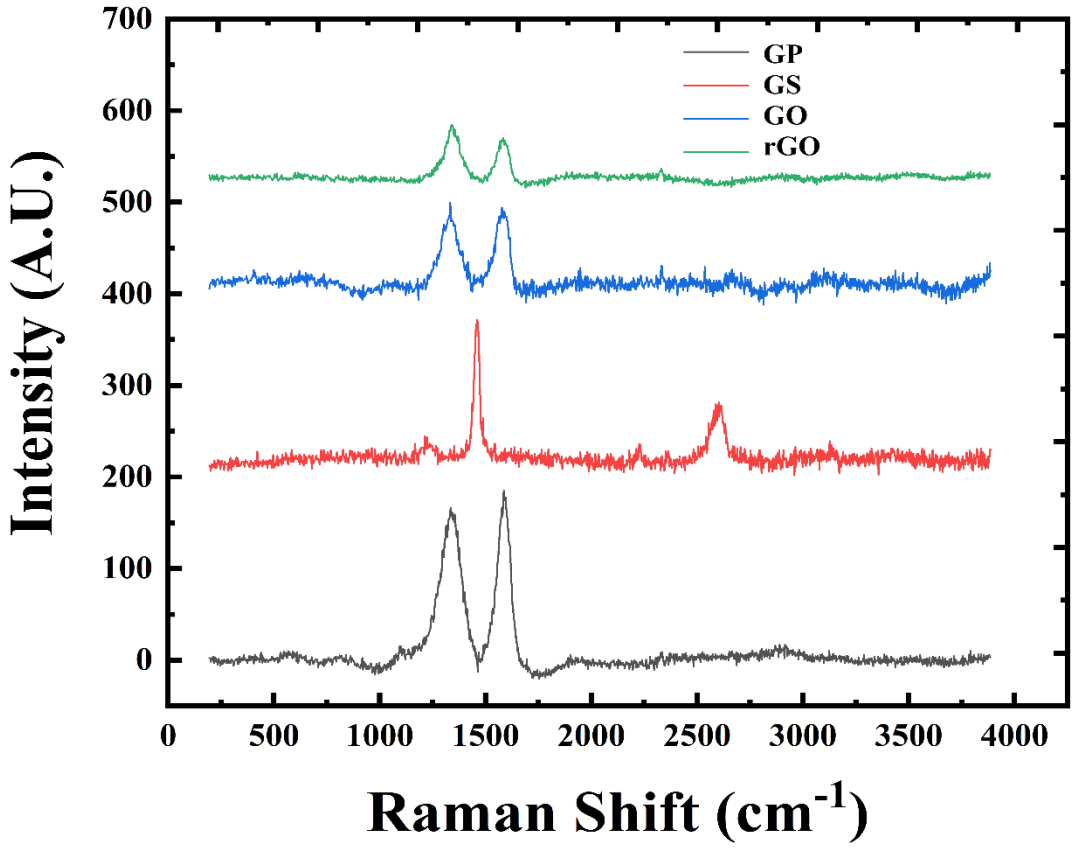

Fig 6. Results from Raman spectroscopy of GP, GS, GO and rGO. Two peaks important for Raman spectroscopy are D band (at 1341 cm^{-1}) and G band (1595 cm^{-1}).

4.1.3. FTIR (Fourier Transform Infrared spectroscopy)

We also did FTIR analysis on GNMs for the presence of the sample's carbon and oxygen functional group. FTIR analysis measures the absorption of infrared radiation by the GNMs versus the wavelength. The FTIR spectra were recorded using the FTIR spectrometer range from 0-5000 cm^{-1} to characterize the functional groups. The FTIR spectra of GNMs showed the hydroxyl group's absorption bands at 3410 cm^{-1}, the C=O at 1720 $cm^{-1,}$ and C-O at 1087 cm^{-1}(Poorali & Bagheri-Mohagheghi, n.d.). These points of the spectral bands can further be used to show the presence of an oxygen functional group

on the graphene samples. Again, the FTIR analysis of GP showed the presence of an oxygen functional group in a higher percentage (Himaja et al., 2015), making GP an unsuitable candidate for the adsorption experiment. Thus, similar to Raman, FTIR spectroscopy was used to determine the materials suitable for the adsorption experiment.

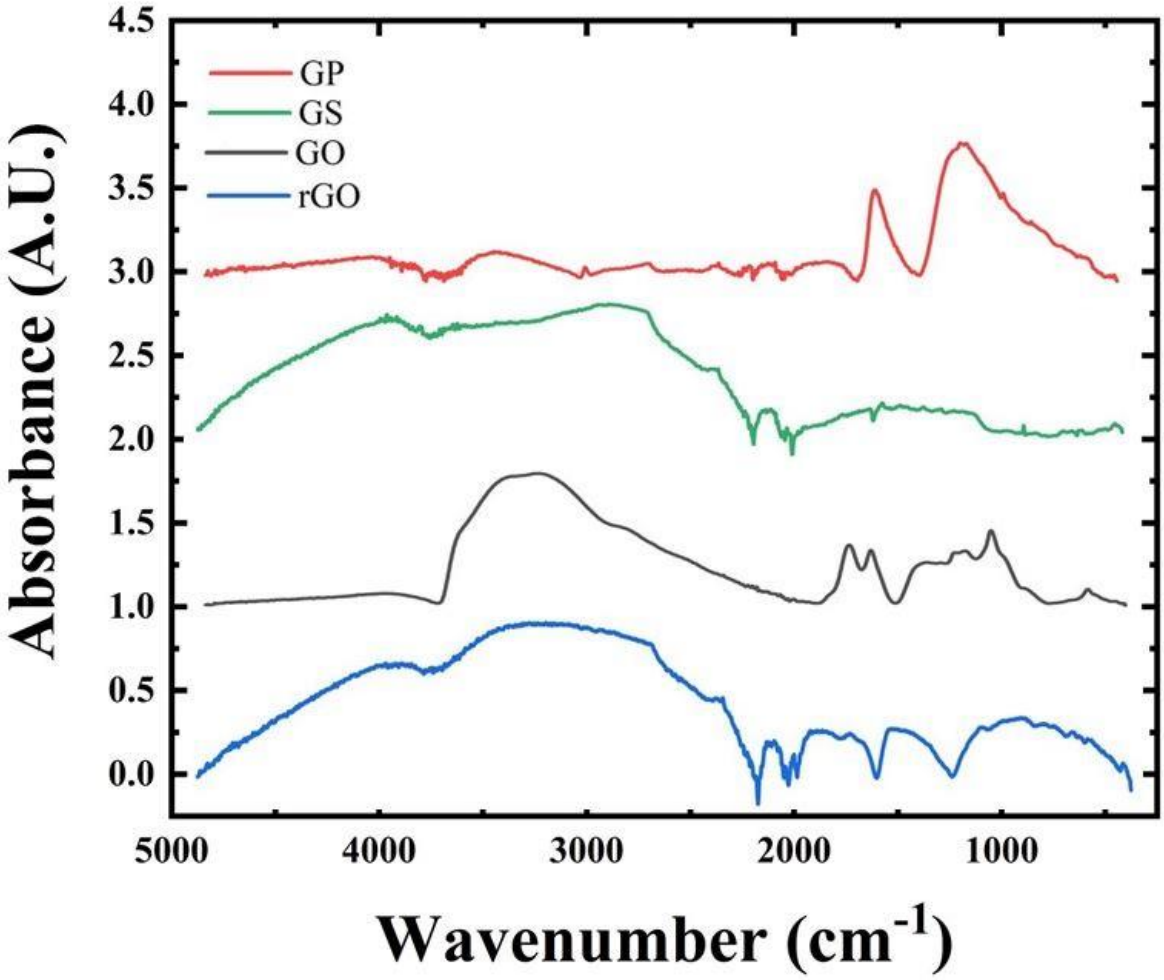

Fig 7. FTIR spectra for GP, GS, GO, and rGO.

4.1.4 Zeta Potential

Zeta Potential is a critical physical property analysis to understand the surface chemistries of NPs, providing information about the electrical state of the charged particles,

which plays an important role in this project. Generally, the values of the zeta potential of material between ±30 mV and ±40 mV are considered to have moderate stability in the colloidal solution (Paar, 2016). In contrast, the NPs with the zeta value range from 0 to ± 10 mV are considered approximately neutral (Pochapski et al., 2021); (Clogston & Patri, 2011).

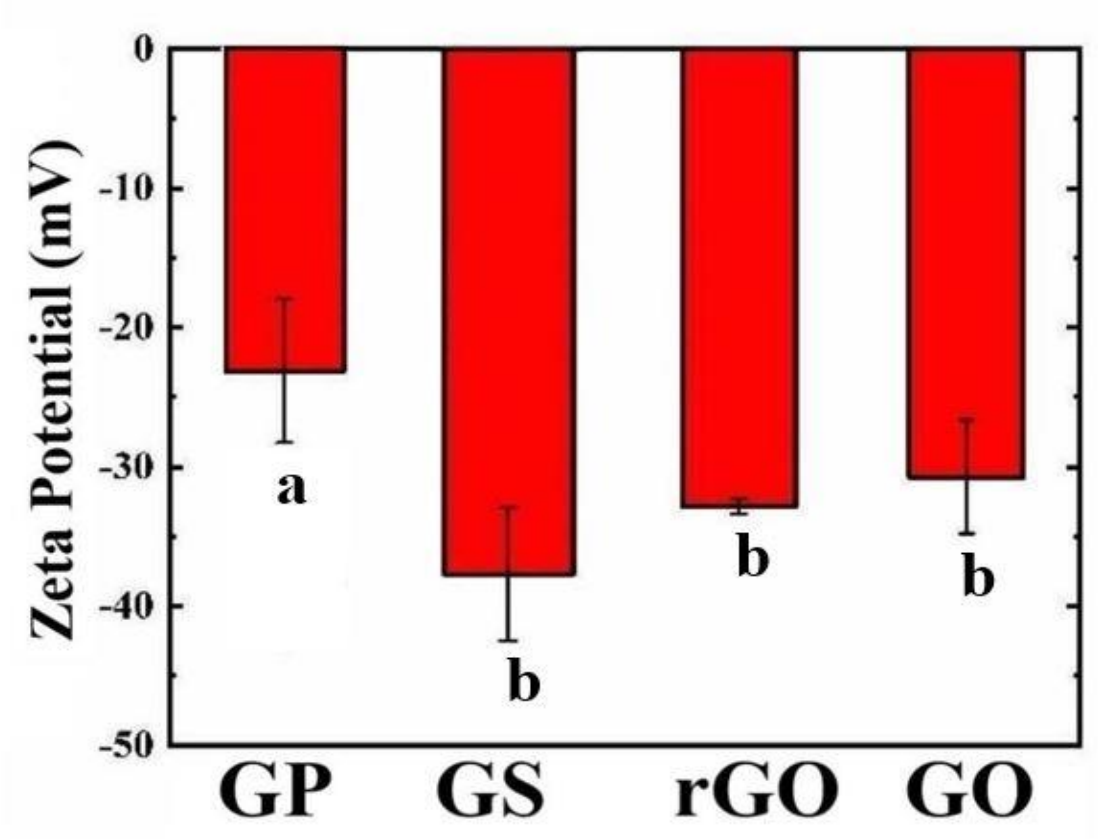

Fig 7. Zeta potential measurement of water dispersed GS, GP, GO, and rGO pH values of 6.5, maintained with the help of 5mM KCl and 0.1 mM of HCO_3. Letters above the bars indicate statistical difference ($p < 0.05$) according to ANOVA.

The zeta potential value was reported as the mean of three replicates. Among the GNMs, the zeta potential value of GS, GO, and rGO always showed values less than -30 mV at all the pH ranges indicating excellent stability of the material in the colloidal solution (Krishnamoorthy et al., 2013) (J. Wang & Chen, 2015). It was also considered that these

three materials would make stable colloidal solutions due to their electrostatic repulsion (Barrios et al., 2019) (Samimi et al., 2018). However, the GP results for zeta potential was around – 23 mV, stating that GP particles are unstable and likely to aggregate (Gholampour et al., 2017) (Bouša et al., 2016). One more reason why we preferred GS for the adsorption experiment rather than GP. However, the absolute value of the zeta potential of GO (Cruces et al., 2021) is higher than rGO; the reason is the lesser oxygen functional groups in rGO (Konkena & Vasudevan, 2012); (Mindivan, 2016).

4.2. Adsorption Isotherms

From the analysis of the adsorption experiment, isotherms were generated to understand the interaction between macro-nutrients and GNMs at room temperature. To keep the parameters same we kept the concentration of adsorbent to be at 1 mg/mL. After adding adsorbate to the solution, the glass vials were sealed, and the samples were agitated for 48 hours for enough reaction time to reach equilibrium. The final readings were an average of three replicate tests at the same parameters. For the adsorption experiments, a negative control was solution graphene sample and DI; for positive control, we used the chemical (used to provide macro-nutrients) and DI water; for a blank solution, we added DI water to the testing kit. The adsorption capacity is computed by:

$$\boldsymbol{qe}\ (\boldsymbol{mg/gm})\ =\ [(\boldsymbol{Co}\ -\ \boldsymbol{Ce})\ /\boldsymbol{m}]\ \boldsymbol{x}\ \boldsymbol{V}$$

4.2.1 Adsorption isotherms for nitrogen nutrients

The adsorption isotherm of GNMs and N nutrient interaction was generated to understand further how N nutrient affinity changes with the change in oxygen content of GNMs. The adsorption results data were well fitted to the Langmuir model (Fig. 8), with

an R^2 values shown in table 4. Even though different concentrations of the adsorbate were used, it is evident that none of the adsorbent reached full saturation. This may be because of the surface area and higher number of active sites of the GNMs for adsorption. Another inference is that GNMs favor the adsorption of N nutrient over their surface up to the maximum concentration (64 mg/L), the upper concentration of adsorbate for the experiment.

Table 4. Plot between GS, GO and rGO for N nutrients after completion of the adsorption period of 48 hours. The R^2 shows the linear regression fit of the plot between GNMs and N nutrients.

Samples	R^2
GS	0.993
GO	0.952
rGO	0.997

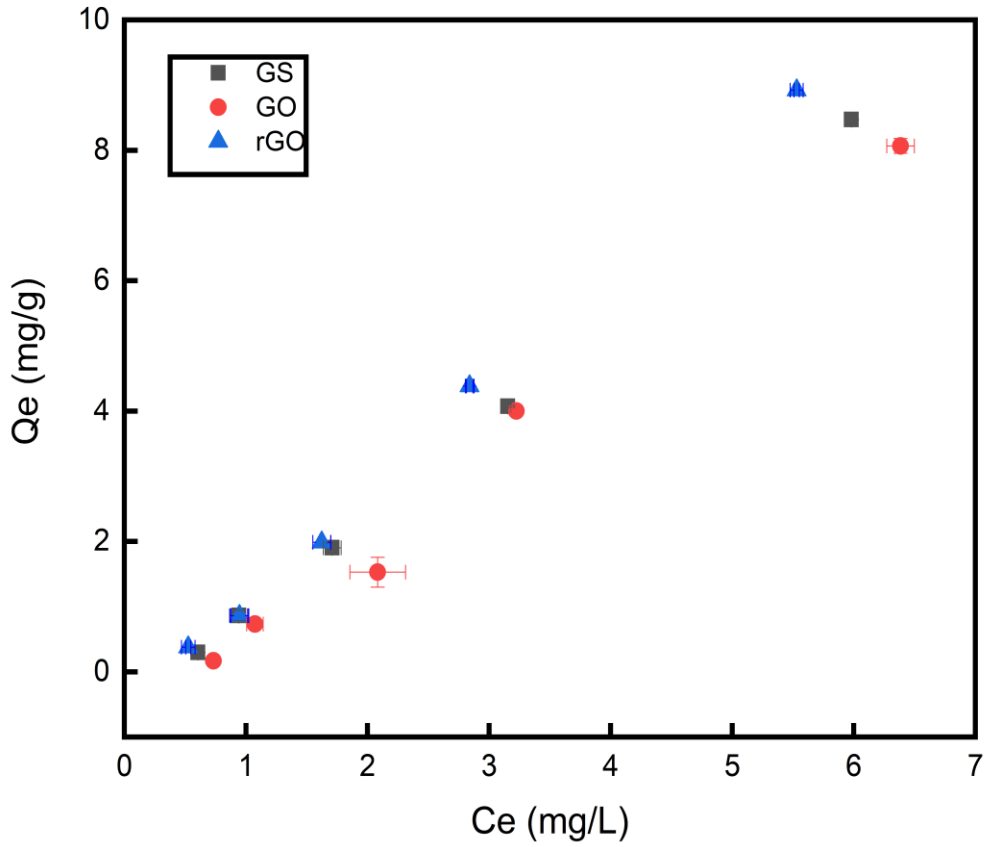

Fig 8. Adsorption Isotherm for N nutrient over GS, GO, and rGO, with the concentration of the adsorbent at 1 mg/mL

4.2.2 Adsorption isotherm for Potassium nutrient

The adsorption isotherm indicated how efficiently the adsorbate will get adsorbed over the GNMs. However, we got the similar adsorption isotherms curves as that in case of nitrate ions. This proves our first hypothesis of the project wrong, that surface charge of the materials will play a major role in adsorption process, because overall charge on nitrate ion is negative and that of potassium is positive. From the plot, it can be observed that there is strong adsorption between the GNMs and K nutrients, and the data fitted well with

Langmuir isotherm with R^2 indicated in table 5. Moreover, it can be noted from the plot that none of the plots has not reached the plateau, meaning that none of the adsorbent sites has reached the saturation limit.

Table 5. Plot for GS, GO and rGO versus K macronutrients after completion of adsorption period of 48 hours. The R^2 of the linear regression fit of plot between K nutrients and GNMs

Samples	R^2
Graphene Sheet	0.839
Graphene Oxide	0.937
Reduced Graphene Oxide	0.935

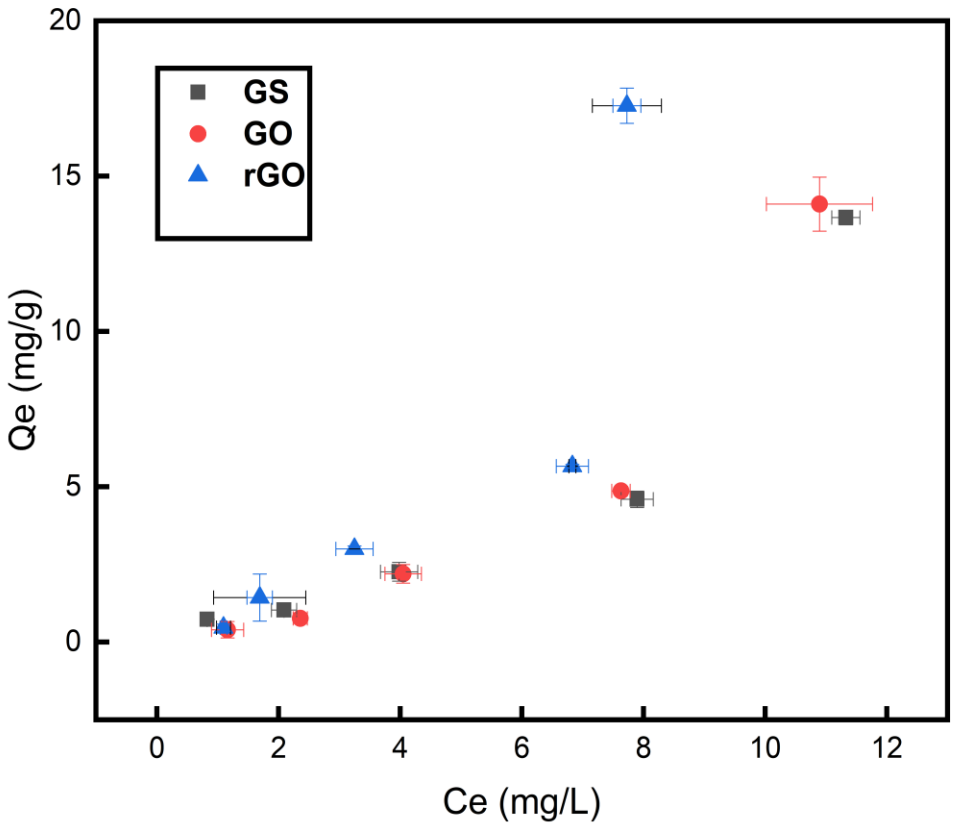

Fig 9. Adsorption Isotherms plotted for asorption experiment between GNMs and K Nutrients with the adsorbent concentration of 1 mg/mL

4.2.3 Adsorption isotherm for Phosphorus nutrient

Results and plot of the P-isotherm are shown in fig. 9. Also, table 6 shows the R^2 value of fitting curves. The plot suggested that the Langmuir model can better describe the fit of the three materials. It can also be observed that the plot of results between GS, rGO, and P nutrients was similar to that of interaction between GNMs and previous nutrients but in the case of GO versus P nutrients, the interaction can be divided into two adsorption stages. First is rapid adsorption because the nutrients initially occupy the active sites of GO; then, as the concentration of adsorbate is increased, nutrients get access to the basal plane of GO, thereby leading to a slower rate of adsorption at higher concentration of adsorbate.

Table 6. Values of GS, GO, and rGO for P macronutrients after completion of the adsorption period of 48 hours. The R^2 of the linear regression fit of plot between P nutrients and GNMs

Samples	R^2
Graphene Sheet	0.98342
Graphene Oxide	0.85634
Reduced Graphene Oxide	0.98173

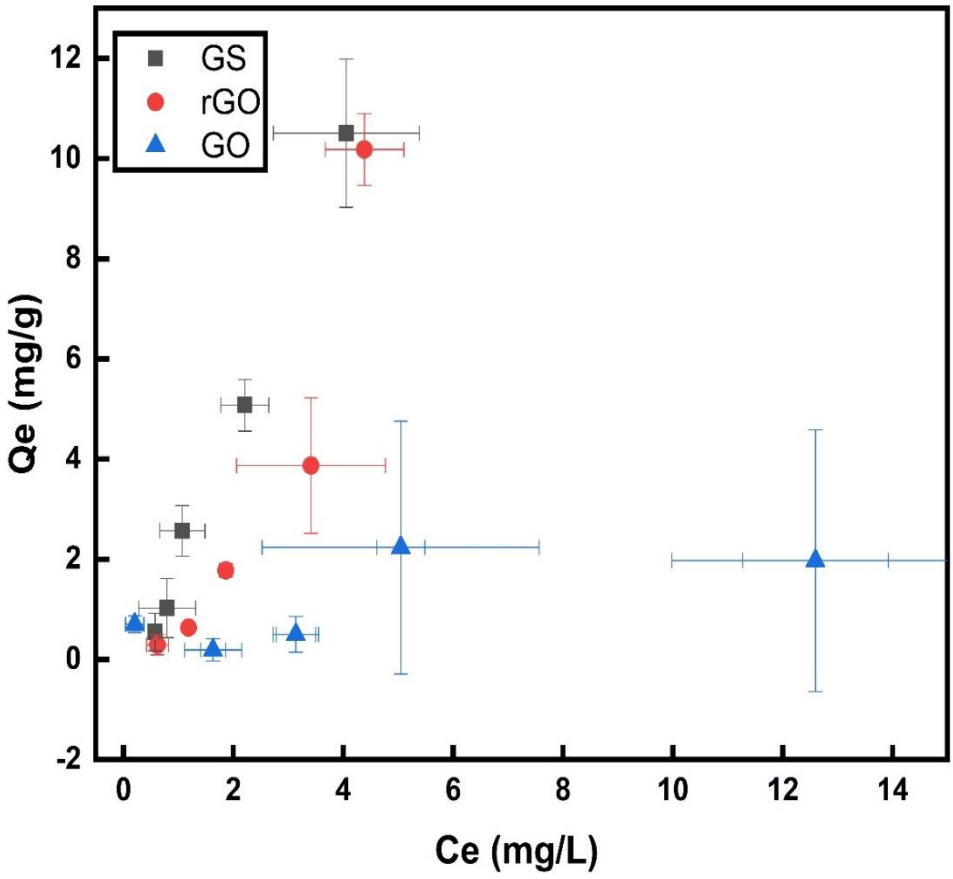

Fig 10. Adsorption isotherm for the interaction between P Nutrients and GNMs with the adsorbent concentration of 1 mg/mL

4.3 Germination assay

We studied the effect of the presence of GO in the germination assay of wheat crops with four different concentrations of GO, namely 20 mg/L, 40 mg/L, 60 mg/L, and 80 mg/L. In addition, we took another set of readings of seed germination without any GO, which serves as a control for our experiment. After completion of the germination period, we observed a higher germination rate than the control. One of the reasons for increased

germination of wheat seeds in the presence of GNMs can be correlated to higher water uptake of the seeds compared to seedlings without GNMs. It was confirmed by analyzing the roots' volume and dry weight, where the root's dry weight was done after oven drying at 50 °C for 48 hours. The measurement was done twice during the experiment, one week and another after three weeks. We also checked the root volume and the chlorophyll content of the seeds better to understand the effect of GO on wheat germination. The findings of the experiments are shown in fig 10. The data were further statistically analyzed with the help of a one-way analysis of variance (ANOVA). In addition, Duncan's post-hoc analysis was used to evaluate the significance of means at $P < 0.05$.

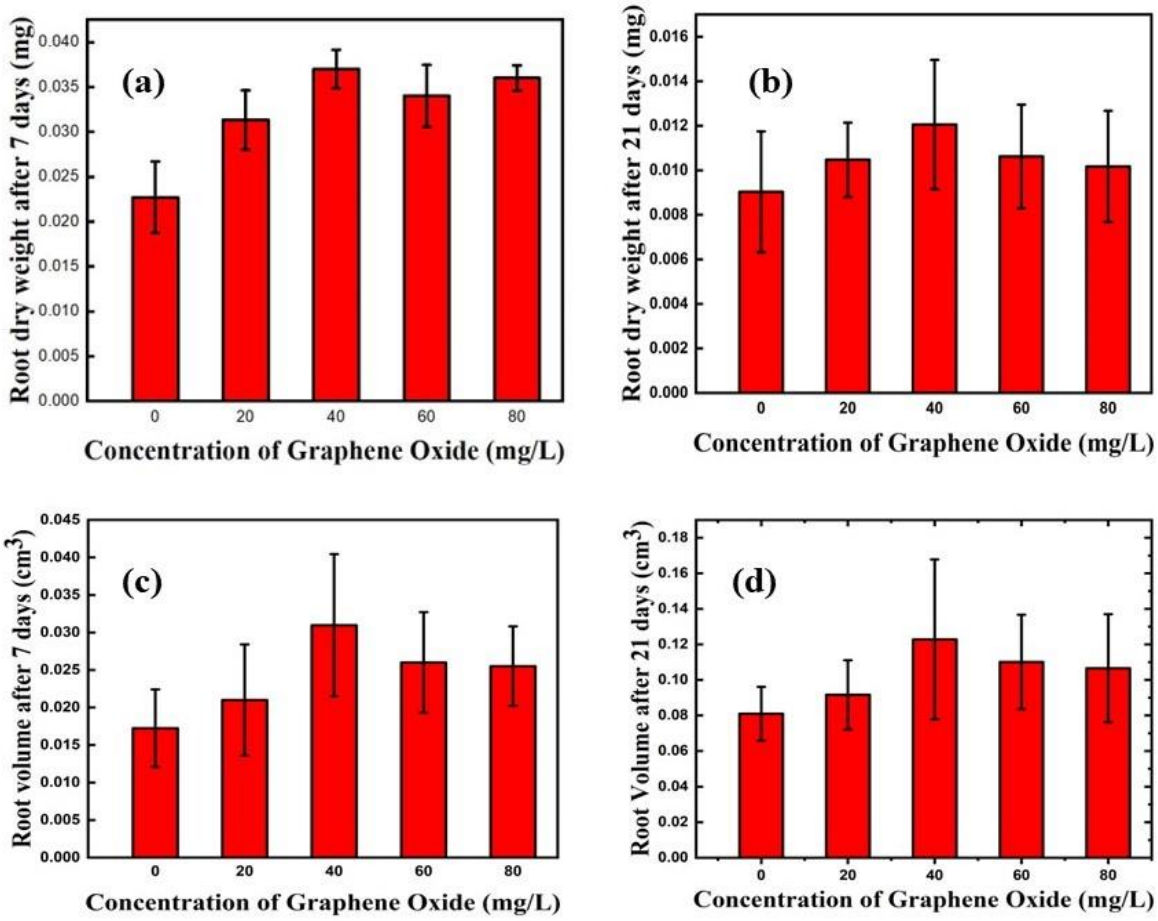

Fig 11. Overall result from germination assay. (a), (b) weight of dry root after one week and three weeks of wheat plant grown with different concentrations of GO. (c), (d) volume of the root system after one week and three weeks, respectively, at different GO concentrations.

From figure 10, it is evident that among the different GONMs concentrations used for the wheat germination analysis, a higher value of dry weight roots was observed at GO concentration of 40 mg/L at the end of the first and third week. A similar trend was observed in the case of root volume at the same concentration of GONMs. For the root system, an average increase in the weight and volume can be observed for seedlings grown in NMs enriched medium as compared to control seedlings grown in the media. There was not much difference in chlorophyll content of the seedlings having GO as compared to the control seedlings. Results of the chlorophyll analysis can be found in figure 11.

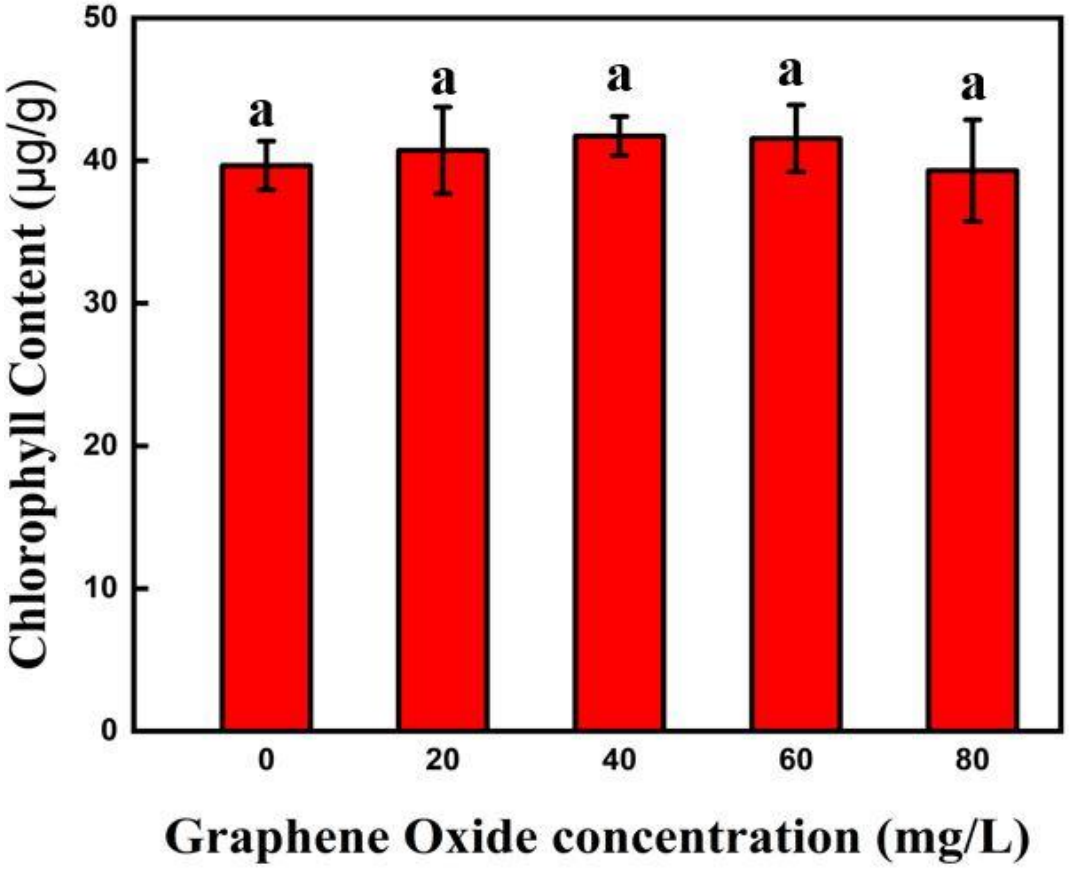

Fig 12. Comparison between the chlorophyll content of the wheat plants after the completion of a 3-week analysis. Letters above the bars indicate statistical difference ($p < 0.05$) according to ANOVA.

Chapter 5

Conclusion

Current agricultural constraints include farmland shrinkage, imbalanced fertilizer application, and low soil nutrient content. In this study, we looked at the interaction between macronutrients and GNMs. GNMs can provide a platform for the controlled release of nutrients when employed in the agricultural field. The results did not suggest any clear relationship between the percentage of the oxygen content of GNMs and the adsorption capacity of the nutrient. However, the study showed that the GNMs favor the N, P, and K nutrients' adsorption. Therefore, GO seems to be the most effective choice amongst the three materials because it has lower production costs than graphene or rGO. Furthermore, the results of the germination assay indicated that the roots' weight and volume were significantly improved with the use of GO in the germination assay, although not in a dose-dependent manner. Overall, the use of GNMS in the implementation in the agricultural field will lead to better utilization of the resources for optimal growth of the crops.

REFRENCES

Aacharya, R., & Chhipa, H. (2020). Nanocarbon fertilizers: Implications of carbon nanomaterials in sustainable agriculture production. *Carbon Nanomaterials for Agri-Food and Environmental Applications*, 297–321. https://doi.org/10.1016/B978-0-12-819786-8.00015-3

Andelkovic, I. B., Kabiri, S., Tavakkoli, E., Kirby, J. K., McLaughlin, M. J., & Losic, D. (2018). Graphene oxide-Fe(III) composite containing phosphate – A novel slow release fertilizer for improved agriculture management. *Journal of Cleaner Production*, *185*, 97–104. https://doi.org/10.1016/j.jclepro.2018.03.050

Arora, S., Sharma, P., Kumar, S., Nayan, R., Khanna, P. K., & Zaidi, M. G. H. (2012). Gold-nanoparticle induced enhancement in growth and seed yield of Brassica juncea. *Plant Growth Regulation*, *66*(3), 303–310. https://doi.org/10.1007/S10725-011-9649-Z

Awasthi, A., Bansal, S., Jangir, L. K., Awasthi, G., Awasthi, K. K., & Awasthi, K. (2017). Effect of ZnO Nanoparticles on Germination of Triticum aestivum Seeds. *Macromolecular Symposia*, *376*(1), 1700043. https://doi.org/10.1002/MASY.201700043

Barrena, R., Casals, E., Colón, J., Font, X., Sánchez, A., & Puntes, V. (2009). Evaluation of the ecotoxicity of model nanoparticles. *Chemosphere*, *75*(7), 850–857. https://doi.org/10.1016/J.CHEMOSPHERE.2009.01.078

Barrios, A. C., Cahue, Y. P., Wang, Y., Geiger, J., Puerari, R. C., Matias, W. G., Melegari, S. P., Gilbertson, L. M., & Perreault, F. (2021). Emerging investigator series: a multispecies analysis of the relationship between oxygen content and toxicity in graphene oxide. *Environmental Science: Nano*, *8*(6), 1543–1559. https://doi.org/10.1039/D0EN01264E

Barrios, A. C., Wang, Y., Gilbertson, L. M., & Perreault, F. (2019). Structure-Property-Toxicity Relationships of Graphene Oxide: Role of Surface Chemistry on the Mechanisms of Interaction with Bacteria. *Environmental Science and Technology*, *53*(24), 14679–14687. https://doi.org/10.1021/ACS.EST.9B05057/SUPPL_FILE/ES9B05057_SI_001.PDF

Berg, M. (2017, October). *Environmental Implications of Excess Fertilizer and Manure*

on Water Quality — Publications. https://www.ag.ndsu.edu/publications/environment-natural-resources/environmental-implications-of-excess-fertilizer-and-manure-on-water-quality

Bouša, D., Luxa, J., Mazánek, V., Jankovský, O., Sedmidubský, D., Klímová, K., Pumera, M., & Sofer, Z. (2016). Toward graphene chloride: chlorination of graphene and graphene oxide. *RSC Advances*, *6*(71), 66884–66892. https://doi.org/10.1039/C6RA14845J

Chen, J., Mu, Q., & Tian, X. (2022). Phytotoxicity of graphene oxide on rice plants is concentration-dependent. *Materials Express*, *47*, 22. https://doi.org/10.1166/mex.2019.1538

Choudhary, S., Raheja, N., Kumar, S., Kamboj, M., & Sharma, A. (2018). A review: Pesticide residue: Cause of many animal health problems. *Journal of Entomology and Zoology Studies*, *6*(3), 330–333. https://www.researchgate.net/publication/325314814

Chu, J. (n.d.). *Insulator or superconductor? Physicists find graphene is both | MIT News | Massachusetts Institute of Technology*. Retrieved June 1, 2022, from https://news.mit.edu/2018/graphene-insulator-superconductor-0305

Chua, C. K., & Pumera, M. (2013). Chemical reduction of graphene oxide: a synthetic chemistry viewpoint. *Chemical Society Reviews*, *43*(1), 291–312. https://doi.org/10.1039/C3CS60303B

Clark, J. (2022, April 16). *The Beer-Lambert Law - Chemistry LibreTexts*. https://chem.libretexts.org/Bookshelves/Physical_and_Theoretical_Chemistry_Textbook_Maps/Supplemental_Modules_(Physical_and_Theoretical_Chemistry)/Spectroscopy/Electronic_Spectroscopy/Electronic_Spectroscopy_Basics/The_Beer-Lambert_Law

Clogston, J. D., & Patri, A. K. (2011). Zeta potential measurement. *Methods in Molecular Biology (Clifton, N.J.)*, *697*, 63–70. https://doi.org/10.1007/978-1-60327-198-1_6

Cohen-Tanugi, D., & Grossman, J. C. (2015). Nanoporous graphene as a reverse osmosis

membrane: Recent insights from theory and simulation. *Desalination*, *366*, 59–70. https://doi.org/10.1016/J.DESAL.2014.12.046

Compton, O. C., & Nguyen, S. T. (2010). Graphene oxide, highly reduced graphene oxide, and graphene: Versatile building blocks for carbon-based materials. *Small*, *6*(6), 711–723. https://doi.org/10.1002/SMLL.200901934

Cruces, E., Barrios, A. C., Cahue, Y. P., Januszewski, B., Gilbertson, L. M., & Perreault, F. (2021). Similar toxicity mechanisms between graphene oxide and oxidized multi-walled carbon nanotubes in Microcystis aeruginosa. *Chemosphere*, *265*, 129137. https://doi.org/10.1016/J.CHEMOSPHERE.2020.129137

El-Temsah, Y. S., & Joner, E. J. (2012). Impact of Fe and Ag nanoparticles on seed germination and differences in bioavailability during exposure in aqueous suspension and soil. *Environmental Toxicology*, *27*(1), 42–49. https://doi.org/10.1002/TOX.20610

Ersan, G., Apul, O. G., Perreault, F., & Karanfil, T. (2017). Adsorption of organic contaminants by graphene nanosheets: A review. *Water Research*, *126*, 385–398. https://doi.org/10.1016/J.WATRES.2017.08.010

Faria, A. F., Perreault, F., & Elimelech, M. (2018). Elucidating the Role of Oxidative Debris in the Antimicrobial Properties of Graphene Oxide. *ACS Applied Nano Materials*, *1*(3), 1164–1174. https://doi.org/10.1021/ACSANM.7B00332/SUPPL_FILE/AN7B00332_SI_001.PDF

Fraceto, L. F., Grillo, R., de Medeiros, G. A., Scognamiglio, V., Rea, G., & Bartolucci, C. (2016). Nanotechnology in agriculture: Which innovation potential does it have? *Frontiers in Environmental Science*, *4*(MAR), 20. https://doi.org/10.3389/FENVS.2016.00020/BIBTEX

Gadipelli, S., & Guo, Z. X. (2015). Graphene-based materials: Synthesis and gas sorption, storage and separation. *Progress in Materials Science*, *69*, 1–60. https://doi.org/10.1016/J.PMATSCI.2014.10.004

Ghann, W. E., Kang, H., Uddin, J., Chowdhury, F. A., Khondaker, S. I., Moniruzzaman,

M., Kabir, M. H., & Rahman, M. M. (2019). Synthesis and Characterization of Reduced Graphene Oxide and Their Application in Dye-Sensitized Solar Cells. *ChemEngineering 2019, Vol. 3, Page 7*, *3*(1), 7. https://doi.org/10.3390/CHEMENGINEERING3010007

Gholampour, A., Valizadeh Kiamahalleh, M., Tran, D. N. H., Ozbakkaloglu, T., & Losic, D. (2017). From Graphene Oxide to Reduced Graphene Oxide: Impact on the Physiochemical and Mechanical Properties of Graphene-Cement Composites. *ACS Applied Materials and Interfaces*, *9*(49), 43275–43286. https://doi.org/10.1021/ACSAMI.7B16736/SUPPL_FILE/AM7B16736_SI_001.PDF

Hajdu, I. (2019). *Macronutrients Play a Vital Role In Crop Production - AGRIVI*. https://www.agrivi.com/blog/macronutrients-play-a-vital-role-in-crop-production/

He, Y., Hu, R., Zhong, Y., Zhao, X., Chen, Q., & Zhu, H. (2018). Graphene oxide as a water transporter promoting germination of plants in soil. *Nano Research*, *11*(4), 1928–1937. https://doi.org/10.1007/s12274-017-1810-1

Hidayah, N. M. S., Liu, W. W., Lai, C. W., Noriman, N. Z., Khe, C. S., Hashim, U., & Lee, H. C. (2017). Comparison on graphite, graphene oxide and reduced graphene oxide: Synthesis and characterization. *AIP Conference Proceedings*, *1892*(1), 150002. https://doi.org/10.1063/1.5005764

Himaja, A. L., Karthik, P. S., & Singh, S. P. (2015). Carbon Dots: The Newest Member of the Carbon Nanomaterials Family. *The Chemical Record*, *15*(3), 595–615. https://doi.org/10.1002/TCR.201402090

Inurria, A., Cay-Durgun, P., Rice, D., Zhang, H., Seo, D. K., Lind, M. L., & Perreault, F. (2019). Polyamide thin-film nanocomposite membranes with graphene oxide nanosheets: Balancing membrane performance and fouling propensity. *Desalination*, *451*, 139–147. https://doi.org/10.1016/J.DESAL.2018.07.004

John, D. A., & Babu, G. R. (2021). Lessons From the Aftermaths of Green Revolution on Food System and Health. *Frontiers in Sustainable Food Systems*, *5*(February), 1–6. https://doi.org/10.3389/fsufs.2021.644559

Kabiri, S., Degryse, F., Tran, D. N. H., Da Silva, R. C., McLaughlin, M. J., & Losic, D. (2017). Graphene Oxide: A New Carrier for Slow Release of Plant Micronutrients. *ACS Applied Materials and Interfaces*, *9*(49), 43325–43335. https://doi.org/10.1021/acsami.7b07890

Kayatz, B., Harris, F., Hillier, J., Adhya, T., Dalin, C., Nayak, D., Green, R. F., Smith, P., & Dangour, A. D. (2019). "More crop per drop": Exploring India's cereal water use since 2005. *Science of the Total Environment*, *673*, 207–217. https://doi.org/10.1016/j.scitotenv.2019.03.304

Khodakovskaya, M., Dervishi, E., Mahmood, M., Xu, Y., Li, Z., Watanabe, F., & Biris, A. S. (2009). *Carbon Nanotubes Are Able To Penetrate Plant Seed Coat and Dramatically Affect Seed Germination and Plant Growth*. *3*(10), 45. https://doi.org/10.1021/nn900887m

Kim, H., Kang, S. O., Park, S., & Park, H. S. (2015). Adsorption isotherms and kinetics of cationic and anionic dyes on three-dimensional reduced graphene oxide macrostructure. *Journal of Industrial and Engineering Chemistry*, *21*, 1191–1196. https://doi.org/10.1016/j.jiec.2014.05.033

Konkena, B., & Vasudevan, S. (2012). Understanding aqueous dispersibility of graphene oxide and reduced graphene oxide through p K a measurements. *Journal of Physical Chemistry Letters*, *3*(7), 867–872. https://doi.org/10.1021/JZ300236W/SUPPL_FILE/JZ300236W_SI_001.PDF

Krishnamoorthy, K., Veerapandian, M., Yun, K., & Kim, S. J. (2013). The chemical and structural analysis of graphene oxide with different degrees of oxidation. *Carbon*, *53*, 38–49. https://doi.org/10.1016/J.CARBON.2012.10.013

Li, S. S., Tu, K. H., Lin, C. C., Chen, C. W., & Chhowalla, M. (2010). Solution-processable graphene oxide as an efficient hole transport layer in polymer solar cells. *ACS Nano*, *4*(6), 3169–3174. https://doi.org/10.1021/NN100551J/ASSET/IMAGES/MEDIUM/NN-2010-00551J_0006.GIF

Lines-Kelly, R. (n.d.). *Plant nutrients in the soil*. Retrieved May 31, 2022, from https://www.dpi.nsw.gov.au/agriculture/soils/soil-testing-and-analysis/plant-nutrients

Madurani, K. A., Suprapto, S., Machrita, N. I., Bahar, S. L., Illiya, W., & Kurniawan, F. (2020). Progress in Graphene Synthesis and its Application: History, Challenge and the Future Outlook for Research and Industry. *ECS Journal of Solid State Science and Technology*, *9*(9), 093013. https://doi.org/10.1149/2162-8777/ABBB6F

Mayhew, L. (n.d.). *Understanding Fertilizer and Solubility | EcoFarming Daily*. Retrieved May 31, 2022, from https://www.ecofarmingdaily.com/build-soil/soil-inputs/fertilizers/fertilizer-solubility/

Mejias, J. H., Salazar, F., Pérez Amaro, L., Hube, S., Rodriguez, M., & Alfaro, M. (2021). Nanofertilizers: A Cutting-Edge Approach to Increase Nitrogen Use Efficiency in Grasslands. *Frontiers in Environmental Science*, *9*, 52. https://doi.org/10.3389/FENVS.2021.635114/BIBTEX

Mindivan, F. (2016). *THE SYNTHESIS AND CHARECTERIZATION OF GRAPHENE OXIDE (GO) AND REDUCED GRAPHENE OXIDE (RGO) – STUME Journals*. International Scientific Journals. https://stumejournals.com/journals/mtm/2016/6/32

Mukherjee, A., Majumdar, S., Servin, A. D., Pagano, L., Dhankher, O. P., & White, J. C. (2016). Carbon Nanomaterials in Agriculture: A Critical Review. *Frontiers in Plant Science*, *7*(FEB2016). https://doi.org/10.3389/FPLS.2016.00172

Mukhopadhyay, S. S. (2014). Nanotechnology in agriculture: prospects and constraints. *Nanotechnology, Science and Applications*, *7*(2), 63. https://doi.org/10.2147/NSA.S39409

Nedosekin, D. A., Khodakovskaya, M. V, Biris, A. S., Wang, D., Xu, Y., Villagarcia, H., Galanzha, E. I., Zharov, V. P., Laboratories, N., & Rockefeller, W. P. (2011). *In Vivo Plant Flow Cytometry: A First Proof-of-Concept*. https://doi.org/10.1002/cyto.a.21128

Nile, S. H., Thiruvengadam, M., Wang, Y., Samynathan, R., Shariati, M. A., Rebezov, M., Nile, A., Sun, M., Venkidasamy, B., Xiao, J., & Kai, G. (2022). Nano-priming as emerging seed priming technology for sustainable agriculture—recent developments and future perspectives. *Journal of Nanobiotechnology*, *20*(1), 254. https://doi.org/10.1186/S12951-022-01423-8

Paar, A. (2016). *Zeta potential :: Anton Paar Wiki*. https://wiki.anton-paar.com/us-en/zeta-potential/

Perreault, F., De Faria, A. F., Nejati, S., & Elimelech, M. (2015a). Antimicrobial Properties of Graphene Oxide Nanosheets: Why Size Matters. *ACS Nano*, *9*(7), 7226–7236. https://doi.org/10.1021/ACSNANO.5B02067/SUPPL_FILE/NN5B02067_SI_001.PDF

Pingali, P. L. (2012). Green revolution: Impacts, limits, andthe path ahead. *Proceedings of the National Academy of Sciences of the United States of America*, *109*(31), 12302–12308. https://doi.org/10.1073/PNAS.0912953109

Pochapski, D. J., Carvalho Dos Santos, C., Leite, G. W., Pulcinelli, S. H., & Santilli, C. V. (2021). Zeta Potential and Colloidal Stability Predictions for Inorganic Nanoparticle Dispersions: Effects of Experimental Conditions and Electrokinetic Models on the Interpretation of Results. *Langmuir*, *37*(45), 13379–13389. https://doi.org/10.1021/ACS.LANGMUIR.1C02056/SUPPL_FILE/LA1C02056_SI_001.PDF

Poorali, M.-S., & Bagheri-Mohagheghi, M.-M. (n.d.). Comparison of chemical and physical reduction methods to prepare layered graphene by graphene oxide: optimization of the structural properties and tuning of energy band gap. *Journal of Materials Science: Materials in Electronics*, *27*. https://doi.org/10.1007/s10854-015-3749-x

Prakash, M. G., & Chung, M. (2016). DETERMINATION OF ZINC OXIDE NANOPARTICLES TOXICITY IN ROOT GROWTH IN WHEAT (TRITICUM AESTIVUM L.) SEEDLINGS. *Acta Biologica Hungarica*, *67*(3), 286–296. https://doi.org/10.1556/018.67.2016.3.6

Rai-Kalal, P., & Jajoo, A. (2021). Priming with zinc oxide nanoparticles improve germination and photosynthetic performance in wheat. *Plant Physiology and Biochemistry*, *160*, 341–351. https://doi.org/10.1016/J.PLAPHY.2021.01.032

Rashed, M. N. (2013). Adsorption Technique for the Removal of Organic Pollutants from Water and Wastewater. *Organic Pollutants - Monitoring, Risk and Treatment*. https://doi.org/10.5772/54048

Salih, A. M., Qahtan, A. A., Al-Qurainy, F., & Al-Munqedhi, B. M. (2022). Impact of Biogenic Ag-Containing Nanoparticles on Germination Rate, Growth, Physiological, Biochemical Parameters, and Antioxidants System of Tomato (Solanum tuberosum L.) In Vitro. *Processes 2022, Vol. 10, Page 825*, *10*(5), 825. https://doi.org/10.3390/PR10050825

Samimi, S., Maghsoudnia, N., Eftekhari, R. B., & Dorkoosh, F. (2018). Lipid-Based Nanoparticles for Drug Delivery Systems. *Characterization and Biology of Nanomaterials for Drug Delivery: Nanoscience and Nanotechnology in Drug Delivery*, 47–76. https://doi.org/10.1016/B978-0-12-814031-4.00003-9

Sheka, E. F., Golubev, Y. A., & Popova, N. A. (2020). Graphene Domain Signature of Raman Spectra of sp2 Amorphous Carbons. *Nanomaterials*, *10*(10), 1–22. https://doi.org/10.3390/NANO10102021

Song, N., Gao, X., Ma, Z., Wang, X., Wei, Y., & Gao, C. (2018). A review of graphene-based separation membrane: Materials, characteristics, preparation and applications. *Desalination*, *437*, 59–72. https://doi.org/10.1016/J.DESAL.2018.02.024

Stampoulis, D., Sinha, S. K., & White, J. C. (2009). Assay-dependent phytotoxicity of nanoparticles to plants. *Environmental Science and Technology*, *43*(24), 9473–9479. https://doi.org/10.1021/ES901695C/SUPPL_FILE/ES901695C_SI_001.PDF

The Fertilizer Institute. (2014, May 7). *Fertilizer 101: The Big 3 - Nitrogen, Phosphorus and Potassium*. The Fertilizer Institute. https://www.tfi.org/the-feed/fertilizer-101-big-3-nitrogen-phosphorus-and-potassium%0Ahttps://www.tfi.org/the-feed/fertilizer-101-big-3-nitrogen-phosphorus-and-potassium#:~:text=Nitrogen%2C phosphorus and potassium%2C or,key role in plant nutrition.

Usman, M., Farooq, M., Wakeel, A., Nawaz, A., Cheema, S. A., Rehman, H. ur, Ashraf, I., & Sanaullah, M. (2020). Nanotechnology in agriculture: Current status, challenges and future opportunities. *Science of The Total Environment*, *721*, 137778. https://doi.org/10.1016/J.SCITOTENV.2020.137778

Vochita, G., Oprica, L., Gherghel, D., Mihai, C. T., Boukherroub, R., & Lobiuc, A. (2019). Graphene oxide effects in early ontogenetic stages of Triticum aestivum L. seedlings. *Ecotoxicology and Environmental Safety*, *181*, 345–352.

https://doi.org/10.1016/J.ECOENV.2019.06.026

Wang, H., Mi, X., Li, Y., & Zhan, S. (2020). 3D Graphene-Based Macrostructures for Water Treatment. *Advanced Materials*, *32*(3), 1806843. https://doi.org/10.1002/ADMA.201806843

Wang, J., & Chen, B. (2015). Adsorption and coadsorption of organic pollutants and a heavy metal by graphene oxide and reduced graphene materials. *Chemical Engineering Journal*, *281*, 379–388. https://doi.org/10.1016/J.CEJ.2015.06.102

Xiong, X., Ji, N., Song, C., & Liu, Q. (2015). Preparation Functionalized Graphene Aerogels as Air Cleaner Filter. *Procedia Engineering*, *121*, 957–960. https://doi.org/10.1016/J.PROENG.2015.09.062

Zhang, H. (2017). *Cause and Effects of Soil Acidity | Oklahoma State University*. https://extension.okstate.edu/fact-sheets/cause-and-effects-of-soil-acidity.html

Zhou, S., & Bongiorno, A. (2013). Origin of the Chemical and Kinetic Stability of Graphene Oxide. *Scientific Reports 2013 3:1*, *3*(1), 1–7. https://doi.org/10.1038/srep02484